



## Flow of Non-Newtonian Fluid in Curved Duct with Varying Aspect Ratio

Hadi A. M., Fathi S. A., Zainy A.

Department of Mathematics, College of Science, University of Baghdad, Baghdad, Iraq.

Received: 4/4/2005 Accepted: 31/10/2005

### Abstract

In this study consideration is given to viscous, incompressible, second order fluid flowing in a rectangular duct, with varying aspect ratio, under the action of the pressure gradient. In particular consideration is given to visco-inelastic liquid. An orthogonal coordinates system has been framed to describe the fluid motion and it is found that the motion equations are controlled by two parameters namely; Dean number and the Non-Newtonian parameter. Solutions for the secondary flow and the axial velocity are derived as perturbations over straight pipe appearing through the dean number. The finite-difference method is employed to find a perturbation solution. These solutions have been developed in certain coordinates for harmonic and biharmonic equations. This study ended with the effect of the non-dimensional and aspect ratio parameters mentioned above on the secondary motion.

### المستخلص

في هذا البحث سنقوم بدراسة مائع لزج غير قابل للانضغاط من الرتبة الثانية ينساب داخل قناة ذات مقطع عرضي مستطيل باختلاف تناسب الأبعاد وتحت تأثير ضغط مترج، وبصورة خاصة الدراسة أخذت لسائل لزج وغير مرن والذي يمثل بمعادلة الحالة والتي بالشكل  $T_{IK} = 2\eta e_{IK} + 4\xi e_{\nu} e_{IK}$  حيث  $\eta$ ،  $\xi$  عبارة عن ثوابت للمائع  $e_{\nu}$  و  $T_{IK}$  هما مركبات الاجهاد ومعدل المرونة على التوالي. نظام الحدائيات المتعامدة تم استخدامه لوصف حركة المائع وقد وجد ان هذه الحركة يتم التحكم بها بواسطة معلمتان هما رقم دين ومعلمة اللانويوتنيين. الحلول للجريان الثنائي والسرعة المحورية أشتقت كمتغيرات طفيفة على الانبوب المستقيم من خلال ظهور رقم دين. طريقة كاليركن وطريقة الفروقات المنتهية استخدمت لاشتقاق هذه التغيرات الطفيفة. هذه الحلول طورت باستخدام إحداثيات معينة للمعادلتين التوافقية والثانية التوافق.

### 1-Introduction

Fluid mechanics is that branch of applied mathematics that is concerned with behaviour of fluids whether they are in motion or at rest. Fluid is that state of matter, which is capable of changing shape, and is capable of flowing. Each fluid characterized by an equation that relates stress to rate of strain, this equation is known as "State Equation". If this relation is linear then the fluid is called "Newtonian fluid", otherwise the fluid is "non-Newtonian fluid". The fluid that we are concerned with in this study is a non-Newtonian fluid and is characterized by the equation of state of the form:

$$T_{ik} = 2\eta e_{ik} + 4\xi e_{ij} e_{jk}, \quad i, j, k = 1, 2, 3 \dots (1)$$

where  $\eta$  and  $\xi$  are the viscosity coefficient and the normal stress respectively,  $T_{ik}$  and  $e_{ik}$  are the stress and rate of strain tensors respectively [6].

The flow of Newtonian and non-Newtonian fluids has been the subject of extensive theoretical studies for many decades. The problem of fluid motion in a bend has been of broad interest both theoretically and experimentally.

The first theoretical study of the subject was made by Dean (1927,1928) who pointed out that the dynamic similarity of the fully developed flow depends on a non-dimensional parameter

(namely Dean number) 
$$L = \frac{2a^3 V_o^2}{\nu^2 R} = 2 \frac{a}{R} (R_E)^2$$

where  $V_o$  is the mean velocity along the pipe,  $\nu$  is the kinematics viscosity,  $a$  radius of the pipe, which is bent in a circle of radius  $R$  and  $R_E$  is the Reynolds's number Dean (1927), [3], introduced a toroidal coordinate system to show that the relation between pressure gradient and the rate of flow through a curved pipe with circular cross-section of incompressible Newtonian fluid is dependant on the curvature. In that paper he could not show this dependence but he did it in his second paper (1928),[4] where he modified his analysis by including higher order terms to be able to show that the rate of flow is slightly reduced by curvature.

Dean and Harst (1957).[5], obtained an approximate solution of Newtonian fluid flow in a curved pipe with rectangular cross- section assuming that the secondary motion is a uniformly stream from inner to outer bend. They modelled the equations of motion by using cylindrical coordinates. This assumption enabled them to obtain Bessel's function solution. They argued that the secondary motion decreases the rate of flow produced by a given pressure gradient and causes an outward movement at the region where the prime motion is the greatest.

In his paper Jones (1960), [6], makes a theoretical analysis of the flow of incompressible Non-Newtonian viscous liquid in a curved pipe with circular cross-section keeping only the first order terms. He shows that the secondary motion consists of two symmetrical vortices and the distance of the streamlines from the central plane decreases as the non-Newtonian parameter increases.

Thomas and Walters (1964), [10, 11], studied flow of an elastic-viscous liquid in a curved pipe with an elliptical cross-section. And they noticed that the liquid elements moves along the pipe in two sets of spirals when the axes of the ellipse in an asymmetrical position. The streamline projections on the cross-section of the pipe are strongly dependant on the elasticity of the liquid. This is not so when the axes are in a symmetrical position. In addition of this the flux through the pipe is independent of the namely Dean and non-Newtonian parameters; also he studied the effect of these two parameters on the secondary flow, axial velocity and some other relations. Our work will be generalized to chapter one of A.M. Ahmad work.

**2-Mathematical model and the governing equations**

Consideration is given to the study of motion of fluid flowing in a curved duct with rectangular cross-section, the position of any point  $Q$  is then specified by cylindrical coordinates  $(x, \theta, z)$ ,  $-a < x < a$  and  $-b < z < b$ . Let  $\alpha = \frac{b}{a}$ , is the aspect ratio. Our analysis concerting on the secondary motion in the case when  $\alpha > 1$ ,  $\alpha < 1$  and  $\alpha = 1$ .

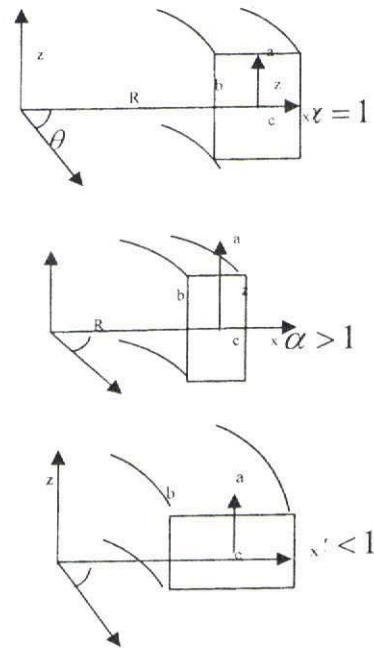


**Fig (1): Coordinates system**

Fig (1) illustrates the coordinates system that has been used, the axis of the circle in which the duct is coiled is OZ formed by the wall of the duct. C is the centre of the section of the duct by a plane through OZ making an angle  $\theta$  with a fixed axial plane. CO is the perpendicular drawn from C upon OZ and is of length R. The plane through O perpendicular to OZ and the line traced out by C will be called the central plane and the centre line of the duct respectively. Cartesian coordinates  $x$  and  $z$  are drawn in the section of the duct where  $x$  is parallel to OC and  $z$  parallel to OZ. The general direction of flow will be taken to be the direction in which  $\theta$  increases. The motion of the fluid is supposed to be due to a fall in pressure along the duct, there will be a fall in pressure if fluid enters the duct from a container at known pressure at one end and flows along the duct to a

container at lower pressure at the other end [1].  
The line elements

$$(ds)^2 = (dx)^2 + (R+x)^2 d\theta^2 + (dz)^2 \dots(2)$$

It is clear that the coordinates form orthogonal coordinates. Thus, one can use definition of the curvilinear coordinates to write down the equations of motion and the continuity equation.

**3-Motion equations and continuity equation**

The full equations of motion and continuity equation for unsteady viscous flow in a curved duct without imposing any restriction are[1]:-

$$\rho \left( \frac{\partial U}{\partial t} + U \frac{\partial U}{\partial x} + \frac{V}{R+x} \frac{\partial U}{\partial \theta} + W \frac{\partial U}{\partial z} - \frac{V^2}{R+x} \right) = -\frac{\partial P}{\partial x} + \frac{\partial T_{xx}}{\partial x} + \frac{1}{R+x} \frac{\partial T_{x\theta}}{\partial \theta} + \frac{\partial T_{xz}}{\partial z} + \frac{T_{xx} - T_{\theta\theta}}{R+x} \dots(3)$$

$$\rho \left( \frac{\partial V}{\partial t} + U \frac{\partial V}{\partial x} + \frac{V}{R+x} \frac{\partial V}{\partial \theta} + W \frac{\partial V}{\partial z} + \frac{UV}{R+x} \right) = -\frac{1}{R+x} \frac{\partial P}{\partial \theta} + \frac{\partial T_{x\theta}}{\partial x} + \frac{1}{R+x} \frac{\partial T_{\theta\theta}}{\partial \theta} + \frac{\partial T_{z\theta}}{\partial z} + \frac{2 T_{x\theta}}{R+x} \dots(4)$$

$$\rho \left( \frac{\partial W}{\partial t} + U \frac{\partial W}{\partial x} + \frac{V}{R+x} \frac{\partial W}{\partial \theta} + W \frac{\partial W}{\partial z} \right) = -\frac{\partial P}{\partial z} + \frac{\partial T_{xz}}{\partial x} + \frac{1}{R+x} \frac{\partial T_{xz}}{\partial \theta} + \frac{\partial T_{zz}}{\partial z} + \frac{T_{xz}}{R+x} \dots(5)$$

$$U \frac{\partial \rho}{\partial x} + \frac{v}{R+x} \frac{\partial \rho}{\partial \theta} + W \frac{\partial \rho}{\partial z} + \rho \left( \frac{\partial U}{\partial x} + \frac{U}{R+x} + \frac{1}{R+x} \frac{\partial v}{\partial \theta} + \frac{\partial W}{\partial z} \right) = 0 \dots(6)$$

Where  $U, V$ , and  $W$  are the velocity components in the direction  $x, \theta$ , and  $z$  respectively. Assume that the motion is steady, the velocity components  $U(x, z), V(x, z), W(x, z)$  are independent of  $\theta$  but  $P$  is not, where  $P$  is the pressure which varies linearly with  $\theta$ . The

dimensions of the cross-section are small in comparison with the radius  $R$ . The components of strain tensor are [1]: -

$$\left. \begin{aligned} e_{xx} &= \frac{\partial U}{\partial x}, \\ e_{\theta\theta} &= \frac{1}{R+x} \left( \frac{\partial V}{\partial \theta} + U \right), \\ e_{zz} &= \frac{\partial W}{\partial z}, \\ e_{\theta z} = e_{z\theta} &= \frac{1}{2} \left( \frac{1}{R+x} \frac{\partial W}{\partial \theta} + \frac{\partial V}{\partial x} \right), \\ e_{zx} = e_{xz} &= \frac{1}{2} \left( \frac{\partial V}{\partial z} + \frac{\partial W}{\partial x} \right), \\ e_{x\theta} = e_{\theta x} &= \frac{1}{2} \left( \frac{\partial V}{\partial x} - \frac{V}{R+x} + \frac{1}{R+x} \frac{\partial U}{\partial \theta} \right) \end{aligned} \right\} \dots(7)$$

Equations of motion and the continuity equation are now modeled on the basis of assumptions mentioned above and we approach non-dimensionalization by introducing the following new quantities

$$\begin{aligned} U &= \frac{v u}{R_h}, V = V_o v, W = \frac{v w}{R_h}, \\ x &= R_h x_1, Z = R_h z_1, \\ P &= \frac{\eta v P^*}{R_h^2}, J = \left( \frac{-R_h^2}{\eta V_o R} \right) \frac{\partial P^*}{\partial \theta} \dots(8) \end{aligned}$$

$$T_{ik} = \frac{\eta v}{R_h^2} \begin{Bmatrix} T'_{xx} & \frac{V_o R_h}{v} T'_{x\theta} & T'_{xz} \\ \frac{V_o R_h}{v} T'_{x\theta} & \left( \frac{V_o R_h}{v} \right)^2 T'_{\theta\theta} & \frac{V_o R_h}{v} T'_{z\theta} \\ T'_{xz} & \frac{V_o R_h}{v} T'_{z\theta} & T'_{zz} \end{Bmatrix}$$

where  $R_h$  is the hydraulic radius. And  $v = \eta / \rho$ ,  $V_o$  is the value of  $V$  at the central line.

**4-Non-dimensional form of the motion equations**

By using equations (1-8), the motion and continuity equations in dimensionless form are

$$u \frac{\partial u}{\partial x_1} + w \frac{\partial u}{\partial z_1} - \frac{1}{2} L v^2$$

$$\begin{aligned}
 &= -\frac{\partial P^*}{\partial x_1} + 2\frac{\partial^2 u}{\partial x_1^2} + 8\beta\left(\frac{\partial u}{\partial x_1}\right)\left(\frac{\partial^2 u}{\partial x_1^2}\right) \\
 &+ 2\beta\left(\frac{\partial u}{\partial z_1} + \frac{\partial w}{\partial x_1}\right)\left(\frac{\partial^2 u}{\partial x_1 \partial z_1} + \frac{\partial^2 w}{\partial x_1^2}\right) + \\
 &\left(\frac{\partial^2 u}{\partial z_1^2} + \frac{\partial^2 w}{\partial z_1 \partial x_1}\right) + 2\beta\left(\frac{\partial^2 u}{\partial z_1 \partial x_1}\left(\frac{\partial u}{\partial z_1} + \frac{\partial w}{\partial x_1}\right) + \right. \\
 &\left. \left(\frac{\partial u}{\partial x_1}\right)\left(\frac{\partial^2 u}{\partial z_1^2} + \frac{\partial^2 w}{\partial z_1 \partial x_1}\right)\right) \\
 &+ 2\beta\left(\frac{\partial^2 w}{\partial z_1^2}\left(\frac{\partial u}{\partial z_1} + \frac{\partial w}{\partial x_1}\right) + \left(\frac{\partial w}{\partial z_1}\right)\right) - \\
 &\left(\frac{\partial^2 u}{\partial z_1^2} + \frac{\partial^2 w}{\partial z_1 \partial x_1}\right) \\
 &\frac{1}{2}\beta L\left(\frac{\partial v}{\partial x_1}\right)^2 - \frac{1}{2}\beta L\left(\frac{\partial v}{\partial z_1}\right)^2 \quad \dots(9)
 \end{aligned}$$

$$u \frac{\partial v}{\partial x_1} + w \frac{\partial v}{\partial z_1} =$$

$$\begin{aligned}
 &J + \frac{\partial^2 v}{\partial x_1^2} + 2\beta\left(\frac{\partial^2 u}{\partial x_1^2}\left(\frac{\partial v}{\partial x_1}\right) + \right. \\
 &\left. \left(\frac{\partial u}{\partial x_1}\right)\left(\frac{\partial^2 v}{\partial x_1^2}\right)\right) \\
 &+ \beta\left(\left(\frac{\partial^2 u}{\partial x_1 \partial z_1} + \frac{\partial^2 w}{\partial x_1^2}\right)\left(\frac{\partial v}{\partial z_1}\right) + \left(\frac{\partial u}{\partial z_1} + \frac{\partial w}{\partial x_1}\right)\right) + \left(\frac{\partial^2 v}{\partial z_1^2}\right) \\
 &\left(\frac{\partial^2 v}{\partial x_1 \partial z_1}\right) \\
 &+ \beta\left(\left(\frac{\partial^2 v}{\partial x_1 \partial z_1}\right)\left(\frac{\partial u}{\partial z_1} + \frac{\partial w}{\partial x_1}\right) + \left(\frac{\partial v}{\partial x_1}\right)\right) \\
 &\left(\frac{\partial^2 u}{\partial z_1^2} + \frac{\partial^2 w}{\partial x_1 \partial z_1}\right) \\
 &+ 2\beta\left(\frac{\partial^2 w}{\partial z_1^2} \frac{\partial v}{\partial z_1} + \frac{\partial w}{\partial z_1} \frac{\partial^2 v}{\partial z_1^2}\right) \quad \dots(10)
 \end{aligned}$$

$$u \frac{\partial w}{\partial x_1} + w \frac{\partial w}{\partial z_1} =$$

$$\begin{aligned}
 &-\frac{\partial P^*}{\partial z_1} + \left(\frac{\partial^2 u}{\partial x_1 \partial z_1} + \frac{\partial^2 w}{\partial x_1^2}\right) \\
 &+ 2\beta\left(\left(\frac{\partial^2 u}{\partial x_1^2}\right)\left(\frac{\partial u}{\partial z_1} + \frac{\partial w}{\partial x_1}\right) + \left(\frac{\partial u}{\partial x_1}\right)\right) \\
 &\left(\frac{\partial^2 u}{\partial x_1 \partial z_1} + \frac{\partial^2 w}{\partial x_1^2}\right) \\
 &+ 2\beta\left(\left(\frac{\partial^2 w}{\partial x_1 \partial z_1}\right)\left(\frac{\partial u}{\partial z_1} + \frac{\partial w}{\partial x_1}\right) + \left(\frac{\partial w}{\partial z_1}\right)\right) \\
 &\left(\frac{\partial^2 u}{\partial x_1 \partial z_1} + \frac{\partial^2 w}{\partial x_1^2}\right) \\
 &+ 2\left(\frac{\partial^2 w}{\partial z_1^2}\right) + 2\beta\left(\frac{\partial u}{\partial z_1} + \frac{\partial w}{\partial x_1}\right)\left(\frac{\partial^2 u}{\partial z_1^2} + \frac{\partial^2 w}{\partial x_1 \partial z_1}\right) + \\
 &8\beta\left(\frac{\partial w}{\partial z_1}\right)\left(\frac{\partial^2 w}{\partial z_1^2}\right) \quad \dots(11)
 \end{aligned}$$

$$\frac{\partial u}{\partial x_1} + \frac{\partial w}{\partial z_1} = 0 \quad \dots(12)$$

The non-slip boundary conditions is given by  $u = v = w = 0$ , on the boundary  $x_1 = \mp k$ ,  $z_1 = \mp s$ , where  $k = 1 + \alpha/\alpha$ ,  $s = 1 + \alpha$ .

**5-Stream function form of equations**

It is convenient at this stage to introduce a stream function  $\Psi(x, z)$  which is defined by

$$u = -\frac{\partial \Psi}{\partial z_1}, \quad w = \frac{\partial \Psi}{\partial x_1} \quad \dots(13)$$

satisfy the continuity equation (12)

In what follows we shall omit the index, it is being understood that the variables are non-dimensional form.

Substituting (13) into (9-11) and eliminating  $P^*$  between the first and third equations, then neglecting the terms of second order and arrangement the last equations we get:

$$\begin{aligned}
 \nabla^4 \Psi &= Lv \frac{\partial v}{\partial z} + \left(\frac{\partial \Psi}{\partial x} \frac{\partial}{\partial z} - \frac{\partial \Psi}{\partial z} \frac{\partial}{\partial x}\right) \nabla^2 \Psi - \\
 &\beta L \left(\frac{\partial v}{\partial x}\right) \left(\frac{\partial^2 v}{\partial x \partial z}\right) - \beta L \left(\frac{\partial v}{\partial z}\right) \left(\frac{\partial^2 v}{\partial z^2}\right) \quad \dots(14)
 \end{aligned}$$



where

$$\Omega = v_0 \frac{\partial v_0}{\partial z} - \beta \frac{\partial v_0}{\partial x} \cdot \frac{\partial^2 v_0}{\partial x \partial z} - \beta \frac{\partial v_0}{\partial z} \cdot \frac{\partial^2 v_0}{\partial z^2}$$

On the region R under the corresponding boundary conditions. Notice that the free terms depend on  $v_0$  values, at the same mesh points, at which  $\Psi$  to be calculated.

### 7-Secondary flow

The main feature of the flow in a curved duct is the secondary flow in the cross-section of the curved ducts. Physically the parameter  $L$  (Dean's number) can be considered as the ratio of the centrifugal force induced by circular motion of the fluid to viscous force when a fluid flows through a curved duct. Pressure gradient directed towards the center of curvature, is setup across the duct to balance the centrifugal force arising from curvature. The fluid near the wall of the duct is moving more slowly than the fluid some way from the wall owing to viscosity and therefore require small pressure gradient to balance the local centrifugal force. As a result of these different pressure gradients, the faster-flowing fluid moves outwards, whilst the slower-flowing fluid moves inward.

This flow is known as the secondary flow and it is superposed on the main stream region towards the outer wall and creating a much thicker layer of slowly moving fluid at the inner wall, however, owing the enhanced mixing and momentum transfer due to the secondary flow, the total frictional loss of energy near the wall increases and the fluid experiences more resistance in posing through the duct.

### 8-Streamline projections in the central plane

The motion of the liquid in the central plane of the duct is of special simplicity. If any point on OC then  $z = 0$  and  $-k < x < k$ ,  $\frac{\partial \Psi}{\partial x} = 0$  and

$w$  vanish (i.e. the liquid particles located in the central plane do not possess the  $w$  component of velocity which is responsible of moving them out of the plane  $x = 0$ ). So at any such point the direction of the velocity of the liquid lies in the central plane, this is mean that any particle of the liquid in this plane will not leave it in the subsequent motion. The motion in the upper half of the duct is therefore quiet distinct from that in

the lower half and it is clear that the central plane is the plane of symmetry from the motion.

### Streamline projections on the cross-section

The secondary flow is the main feature of the flow through a curved duct, where is caused by the centrifugal force due to the curved boundaries. Because the centrifugal force intensifies the motion of the fluid particle in a curved duct, the fraction of the flow in a curved duct is higher than a straight one.

The projection of the stream function on the cross-section represented by  $\Psi_1 = \text{constant}$ ,

where  $\Psi_1$  is the solution of equation (18). We analyze many cases to study the effect of the non-Newtonian parameter  $\beta$  and the effect of the aspect ratio  $\alpha$  on the flow in the cross-section of a curved duct. Numerical illustrations are given for a particular boundary and Reynolds number considered by Dean [8], namely:

$$R_h = 63.3 \quad \frac{(R_h)}{R} = \frac{1}{3}$$

and for different values of the parameter  $\alpha$  and  $\beta$ .

Thirty cases are studied to ascertain how the Non-Newtonian parameter and the aspect ratio  $\alpha$

affect the secondary motion in a curved duct. The parameter  $\alpha$  is set at 0.1, 0.5, 1, 2, and 10, and  $\beta$  varies from 0 to 2.1.

Figures (2-7), illustrate the effect of the non-Newtonian parameter  $\beta$  on rectangular cross-section with aspect ratio  $\alpha = 1$ . It is found that as  $\beta$  increase from 0 (Newtonian fluid) to 2.1, the intensity of the secondary flow increases from 0.0005 to 0.3.

The effect of  $\beta$  on a rectangular cross-section with aspect ratio  $\alpha = 2$  is illustrate in figures (8-13), and it is noted that the intensity of the secondary flow increase from 0.0001 to 0.6. The same issue is examined for  $\alpha = 0.5$ , here it found that  $\psi$  increases from 0.0005 to 1, see figures (14-19).

Two more aspect ratios are tested. The first one  $\alpha = 0.1$  (small) in which it is found that the intensity of the secondary flow increased from 0.1 to 40. While in the second one  $\alpha = 10$  (large), the intensity increased from 0.0002 to 0.004, see figures (26-31).

It is noticed that for all  $\alpha$  and  $\beta$ , the nature of stream lines is a closed and symmetric curves in

the upper and lower halves of the cross-sections "i.e. the closed curves obtained is the reflexion in OC", it has already been seen that the motion in two parts into which the duct divided by the central plane are independent with opposite direction.

It is observed that the intensity of secondary flow is stronger in the middle in each secondary vortex and becomes weaker whenever we move towards the boundaries and the central plane, and this intensity increases as  $\beta$  increases, in addition to that, there exists a vertical displacement in the centre of each vortex.

For  $\alpha = 1, 2, 0.5$  Fig (2-19) one can see the effects of the two parameters  $\alpha$  and  $\beta$  for a fixed  $\alpha$  and  $\beta$  varies from 0 to 2.1 then the intensity of the stream function increases and when  $\alpha$  decreases from 2 to 0.5 and  $\beta$  fixed then the intensity increases.

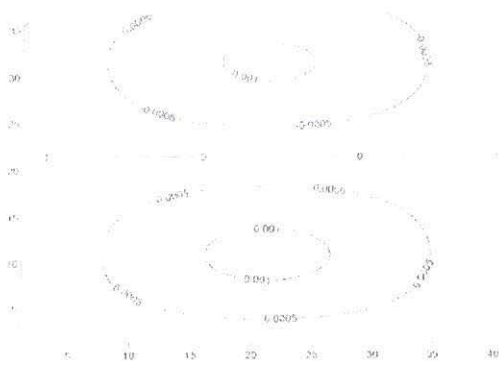
Now, for  $\alpha = 0.1$  (strong wide rectangular region) and  $\beta$  varies from 0 to 2.1 we noticed that there are two symmetric vortices covered the

upper and lower halves of the cross-sections See Fig (20-25).

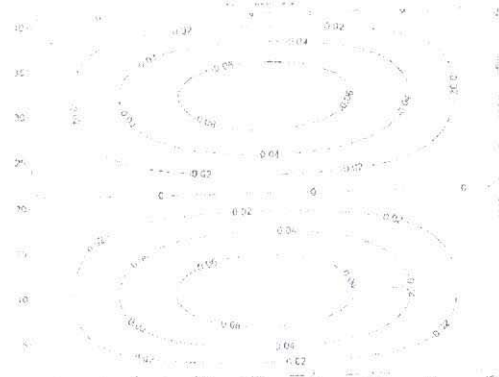
For  $\alpha = 2$ , Fig (8-13), it is observed that there is a stagnation region "the region where all points have a zero velocity" started to appear in the centre of the cross-section near the central plane. The last observations became clearer as  $\alpha$  increases for example when  $\alpha = 10$  see Fig (26-31).

Another feature of the secondary flow, stream lines pattern is the increases in the curvature of the streamlines as  $\alpha$  increases.

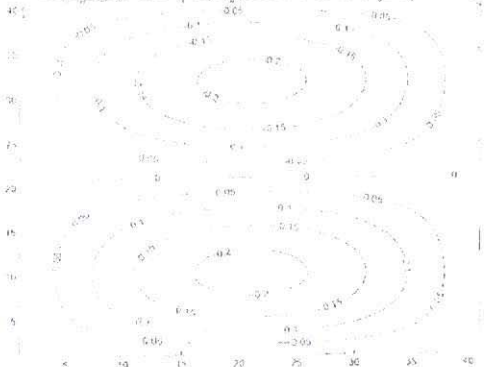
If the scale of the region is taken  $\alpha = 1$  and  $(k/2, s/2)$  we cover the results of non-Newtonian fluid flow in a curved duct with square cross-section [1]. If the non-Newtonian parameter  $\beta$  is set to equal 0 we cover the results of the Newtonian fluid flow in a curved duct with different aspect ratio. If  $L = 0$  then  $\Psi = 0$  then we have flow of Newtonian fluid in a straight duct with different aspect ratio.



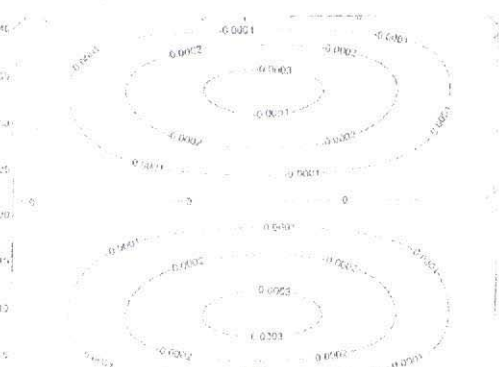
Fig(2) stream lines projection in the cross-section for  $\alpha=1, \beta=0$   $\Psi$  varies from 0.001 to 0.0005.



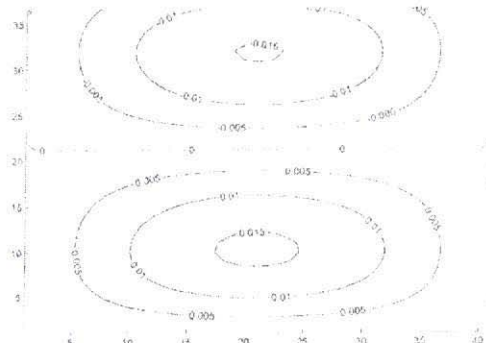
Fig(4) stream lines projection in the cross-section for  $\alpha=1, \beta=0.5$   $\Psi$  varies from 0.06 to 0.02.



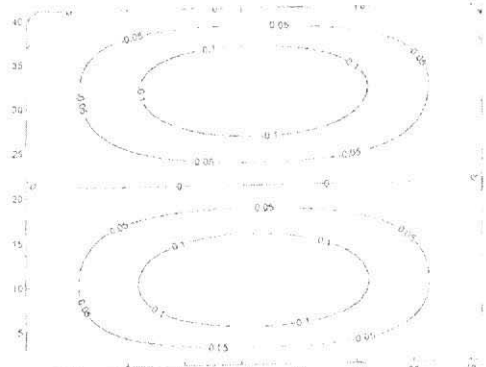
Fig(6) stream lines projection in the cross-section for  $\alpha=1, \beta=1.5$   $\Psi$  varies from 0.02 to 0.05.



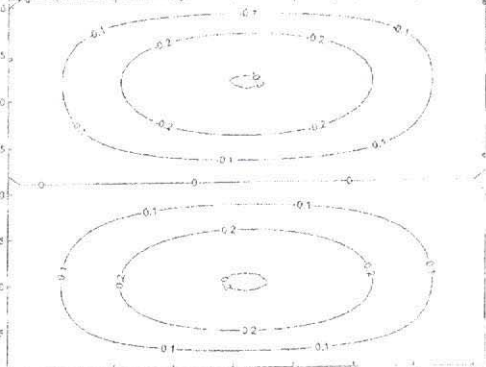
Fig(8) stream lines projection in the cross-section for  $\alpha=2, \beta=0$   $\Psi$  varies from 0.0003 to 0.0001.



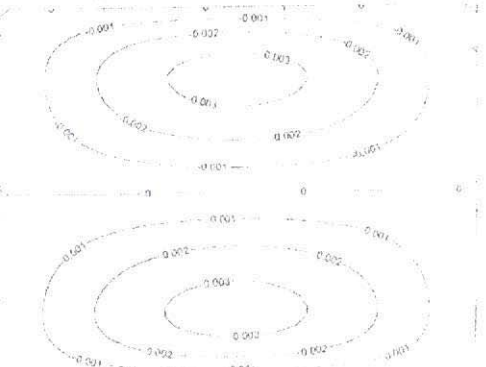
Fig(3) stream lines projection in the cross-section for  $\alpha=1, \beta=0.1$   $\Psi$  varies from 0.015 to 0.0005.



Fig(5) stream lines projection in the cross-section for  $\alpha=1, \beta=1$   $\Psi$  varies from 0.1 to 0.05.

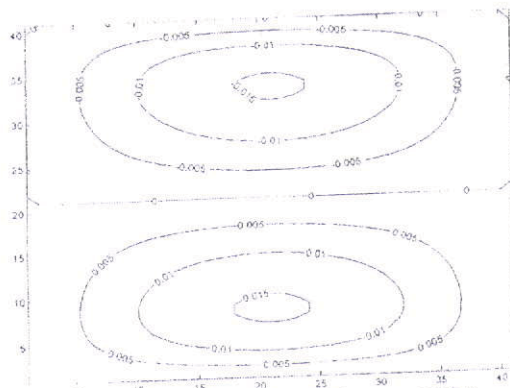


Fig(7) stream lines projection in the cross-section for  $\alpha=1, \beta=2.1$   $\Psi$  varies from 0.3 to 0.1.

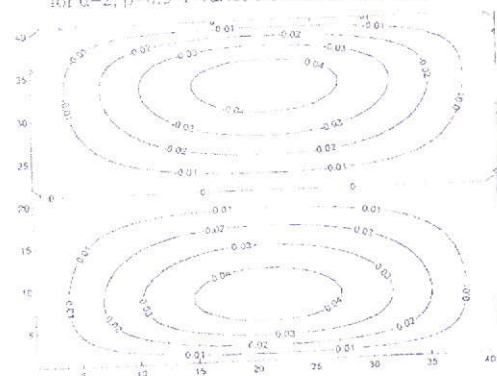


Fig(9) stream lines projection in the cross-section for  $\alpha=2, \beta=0.1$   $\Psi$  varies from 0.003 to 0.001.

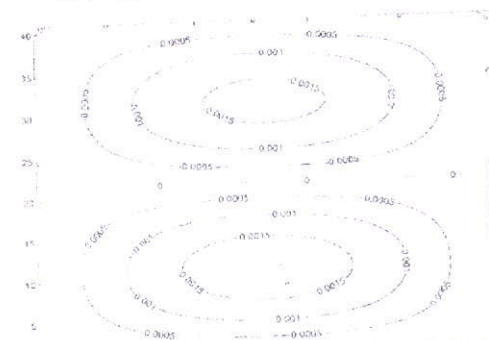




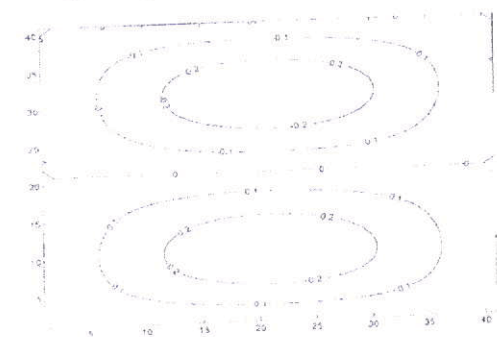
Fig(10) stream lines projection in the cross-section for  $\alpha=2, \beta=0.5$   $\Psi$  varies from 0.015 to 0.005.



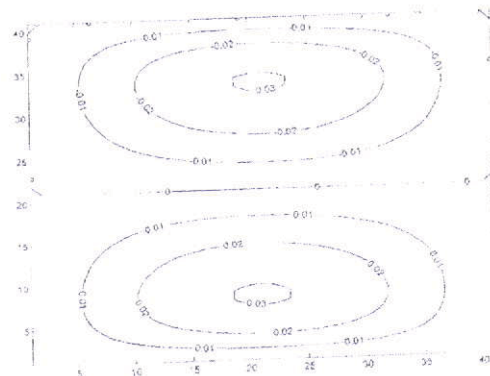
Fig(12) stream lines projection in the cross-section for  $\alpha=2, \beta=1.5$   $\Psi$  varies from 0.04 to 0.01.



Fig(14) stream lines projection in the cross-section for  $\alpha=0.5, \beta=0$   $\Psi$  varies from 0.0015 to 0.0005.



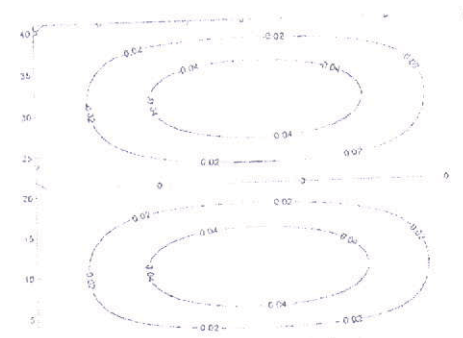
Fig(16) stream lines projection in the cross-section for  $\alpha=0.5, \beta=0.5$   $\Psi$  varies from 0.2 to 0.1.



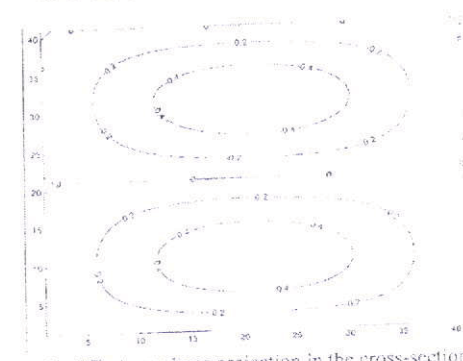
Fig(11) stream lines projection in the cross-section for  $\alpha=2, \beta=1$   $\Psi$  varies from 0.03 to 0.01.



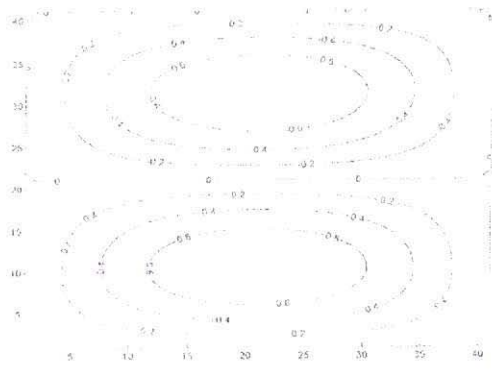
Fig(13) stream lines projection in the cross-section for  $\alpha=2, \beta=2.1$   $\Psi$  varies from 0.06 to 0.02.



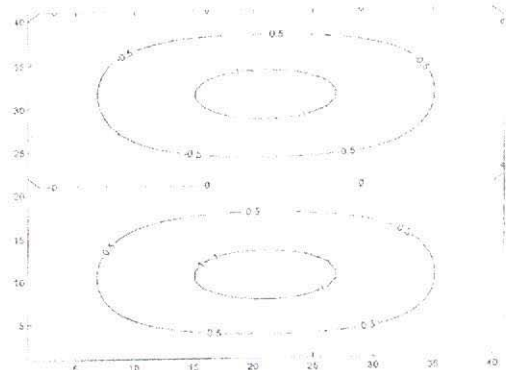
Fig(15) stream lines projection in the cross-section for  $\alpha=0.5, \beta=0.1$   $\Psi$  varies from 0.04 to 0.02.



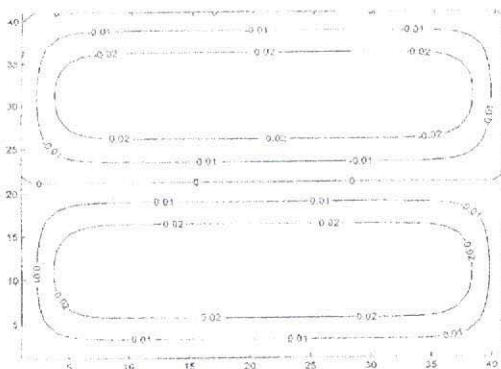
Fig(17) stream lines projection in the cross-section for  $\alpha=0.5, \beta=1$   $\Psi$  varies from 0.4 to 0.2.



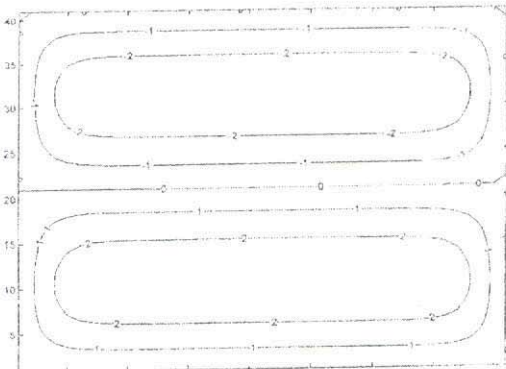
Fig(18) stream lines projection in the cross-section for  $\alpha=0.5$ ,  $\beta=1.5$   $\Psi$  varies from 0.6 to 0.2



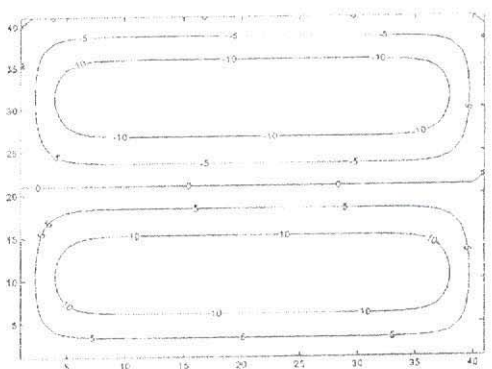
Fig(19) stream lines projection in the cross-section for  $\alpha=0.5$ ,  $\beta=2.1$   $\Psi$  varies from 1 to 0.5



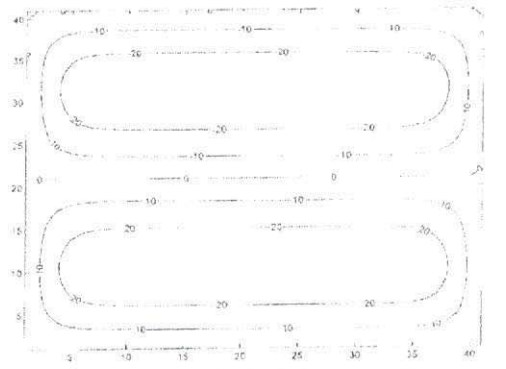
Fig(20) stream lines projection in the cross-section for  $\alpha=0.1$ ,  $\beta=0$   $\Psi$  varies from 0.02 to 0.01.



Fig(21) stream lines projection in the cross-section for  $\alpha=0.1$ ,  $\beta=0.1$   $\Psi$  varies from 2 to 1.



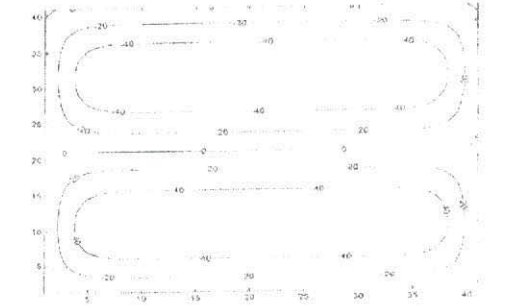
Fig(22) stream lines projection in the cross-section for  $\alpha=0.1$ ,  $\beta=0.5$   $\Psi$  varies from 10 to 5.



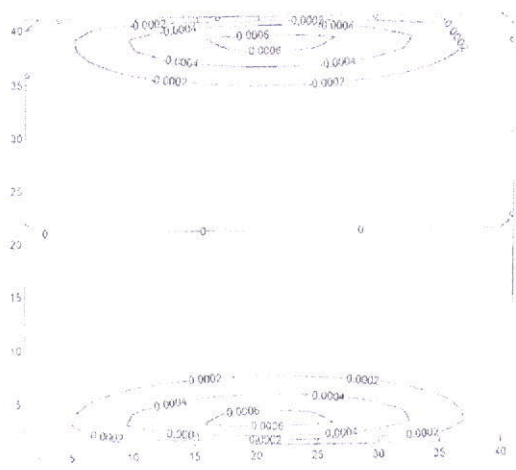
Fig(23) stream lines projection in the cross-section for  $\alpha=0.1$ ,  $\beta=1$   $\Psi$  varies from 20 to 10.



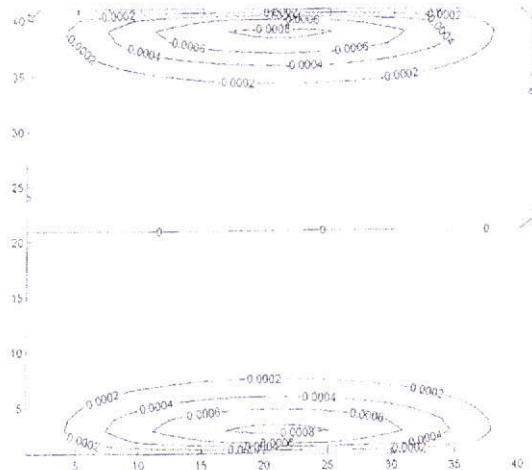
Fig(24) stream lines projection in the cross-section for  $\alpha=0.1$ ,  $\beta=1.5$   $\Psi$  varies from 30 to 10.



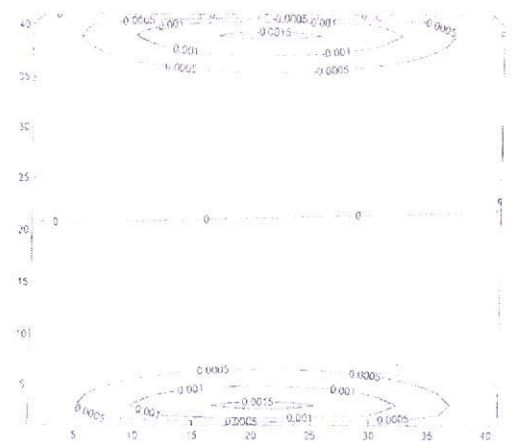
Fig(25) stream lines projection in the cross-section for  $\alpha=0.1$ ,  $\beta=2.1$   $\Psi$  varies from 40 to 20.



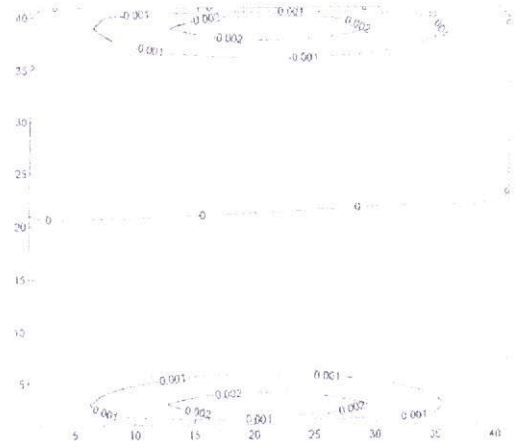
Fig(26) stream lines projection in the cross-section for  $\alpha=10, \beta=0$   $\Psi$  varies from 0.0005 to 0.002.



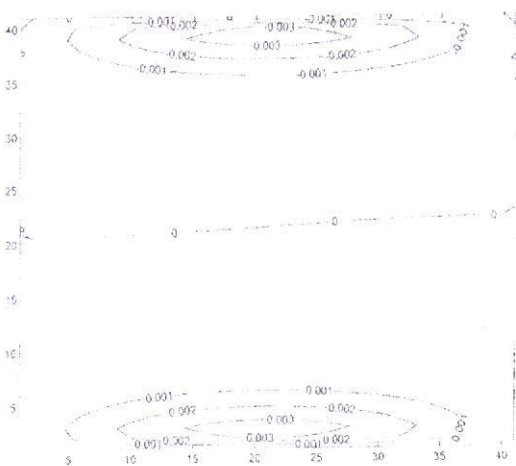
Fig(27) stream lines projection in the cross-section for  $\alpha=10, \beta=0.1$   $\Psi$  varies from 0.008 to 0.0002.



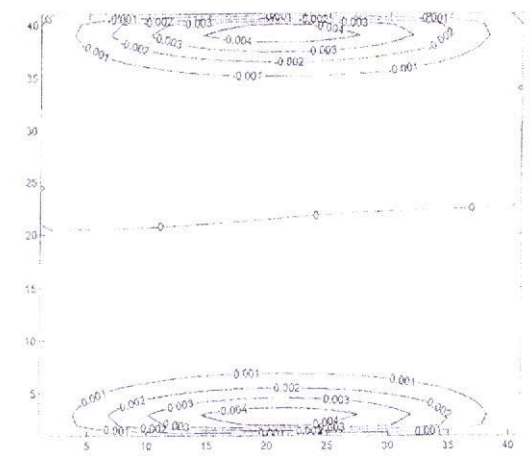
Fig(28) stream lines projection in the cross-section for  $\alpha=10, \beta=0.5$   $\Psi$  varies from 0.0015 to 0.0005.



Fig(29) stream lines projection in the cross-section for  $\alpha=10, \beta=1$   $\Psi$  varies from 0.002 to 0.001.



Fig(30) stream lines projection in the cross-section for  $\alpha=10, \beta=1.5$   $\Psi$  varies from 0.003 to 0.001.



Fig(31) stream lines projection in the cross-section for  $\alpha=10, \beta=2.1$   $\Psi$  varies from 0.004 to 0.001.

## References

- 1-Ahmad M. A. Hadi, "Flow Analysis Through Curved Pipes" PhD. thesis submitted to the university of pune, (2000)
- 2-Cheng K. C., Lin R. C. and Ou J. W., "Fully Developed Laminar Flow In A Curved Rectangular Channel" Trans ASME I; J. Fluids Engng, (1976), Vol. 98 pp 41.
- 3-Dean W. R., "Note On The Motion Of Fluid In A Curved Pipe" Philos. Mag., (1927), Vol. 20. pp. 208.
- 4-Dean W. R., "The Stream Line Motion Of Fluid In A Curved Pipe" Philos. Mag., (1928), Vol. 30, pp. 673.
- 5-Dean W. R. and Hurst J. M., "Note On The Motion Of Fluid In Curved Pipe" Mathematika, (1959) Vol. 6, pp 77.
- 6-Jones J. R., "Flow of a non-Newtonian liquid in a curved pipe" Quart. Journal. Mech. And Applied Math., (1960), Vol. XIII, pt4, pp.428.
- 7-Ravi Sankar S. Nandakumar K. and Masliya J. H., "Oscillatory Flows In Coiled Square Ducts" Phys. Fluids, (1988) Vol. 31 pp 1348.
- 8-Smith G. D. "Numerical Solution Of Partial Differential Equations" (1969), Oxford. University Press.
- 9-Thangam S. and Hur N., "Laminar Secondary Flow In A Curved Rectangular Ducts" J. Fluid Mech., (1990), Vol. 217 pp.421.
- 10-Thomas R. H., Walters k, "On Flow Of An Elastico-Viscous Liquid In A Curved Pipe Under A Pressure-Gradient" J. Fluid Mech., (1962), Vol. 16, pp 228.
- 11-Thomas R. H., Walters K., "On Flow Of An Elastico-Viscous Liquid In A Curved Pipe Of Elliptic Cross-Section Under A Pressure-Gradient" J. Fluid Mech., (1964) Vol.21, part 1, pp. 173.